Analytical Design of Static VAR Compensator-Based Subsynchronous Damping Controller

Shashidhara M Kotian
EEE Department
BITS Pilani K K Birla Goa campus, Zuarinagar
Goa 403726 (Email: shashikotian@gmail.com)

Shubhanga K. N.
EEE Department
NITK-Surathkal,Mangalore
Karnataka 575025 (Email: knsa1234@yahoo.com)

***Abstract*—In this paper, using a dynamic phasor model of static VAR compensator (SVC) a method to determine the phase response of a system analytically is presented. Then using the phase compensation method a subsynchronous damping controller (SSDC) for SVC is designed to mitigate subsynchronous resonance (SSR) in series capacitor compensated power systems. The designed SSDC is validated using detailed time-domain simulations in PSCAD/EMTDC. The case studies are carried out on the IEEE first benchmark system.**

***Keywords*—Dynamic phasor, Eigenvalue analysis, static VAR compensator (SVC), Subsynchronous damping controller (SSDC), Subsynchronous resonance (SSR).**

I. Introduction

Fixed series capacitor (FSC) compensation is the economical means of enhancing the power transfer capacity of long transmission lines. However, such an FSC compensated power system connected to turbo-generator may lead to shaft damage due to subsynchronous resonance (SSR) [1]. SSR occurs when the complement of the electrical natural frequency matches with any of the torsional mode frequencies of the turbine-generator system [2]. This kind of SSR is called as torsional interaction (TI). In [3], using a two-mass model, TI has been demonstrated systematically.

Various countermeasures have been suggested and even some of them have been applied in practice to solve the problem of SSR [4]-[6]. Application of flexible ac transmission systems (FACTS), namely, static VAR compensator (SVC) [7]-[11], thyristor-controlled series capacitor (TCSC) [11]-[16], static synchronous series compensator (SSSC) [17],[18], static synchronous compensator (STATCOM) [19], [20], UPFC [21], etc. for the SSR mitigation has been extensively investigated and reported. Further, it is well established in the literature that these FACTS devices must be provided with a supplementary controller known as subsynchronous damping controller (SSDC) to provide adequate damping for SSR oscillations [9]-[24]. Various techniques such as residue method [16], [25], [26], pole-placement technique [27], modal control theory-based method [28]-[30], eigen-structure assignment technique [31], etc. which have been used to design SSDC demand a complete state-space modeling of the system. Sometimes eigenvalue and time-domain simulation based methods [8], optimization techniques [32]-[34] have been used to obtain the SSDC parameters. SSDC design using these techniques are analytically intensive. However, the well-known phase compensation (PC) technique [16],[23]-[24] is a straightforward method to design SSDC. In this approach, the phase response of the open-loop system needs to be determined. The PC method needs an accurate and reliable analytical model of FACTS devices which is not easy to derive when they involve switching devices like thyristors. Test signal (TS) method [23]-[24] employing detailed time-domain simulations provides accurate phase response. However, this method is computationally demanding and also time-consuming. Using discrete-time (DT) model [16], [27], [35] of FACTS devices the phase angles can be obtained analytically. However, the DT model derivation is complex.

In this paper, the application of a dynamic phasor (DP) model of SVC [9] is proposed to obtain the phase response analytically. The PC technique is employed to design SSDC of an SVC-based SSR mitigation scheme. From various continuous-time (CT) models [36]-[38], in this paper, the DP-based CT model of SVC is used due to its modularity and accuracy. Though the SVC DP models and the SSDC design are not new, this paper discusses the usage of the DP-model of SVC to obtain accurate phase response of the system.

The phase-frequency characteristic obtained using the proposed approach is compared with that determined using the TS method and the designed SSDC is validated using time-domain simulations in PSCAD/EMTDC. In this regard, the paper presents a promising analytical tool alternative to time-domain simulation-based TS method/ DT model-based analytical tool for the SSDC design. All case studies are conducted on the IEEE first benchmark system (FBS) [39].

II. Continuous-Time Model of SVC

In this section, the dynamic phasor model of SVC [9], [40] is presented. Fig. 1 shows the circuit diagram of a single-phase SVC. The model is derived in detail in [40]. The dynamics of phase-locked loop (PLL) is also included in the model.

The state-space model for SVC is given in (1). The switching function, q, denotes the status of thyristor: q=1 when one of the thyristors is on, and q=0 with both thyristors off.

$$C_{TC}\frac{dv}{dt} = i_l - i; \quad L_{TCR}\frac{di}{dt} = qv \tag{1}$$

The DP-model of the SVC for fundamental frequency is given by (2). In (2), V_1 and I_1 denote the fundamental phasors

978-1-5386-2462-3/18/$31.00

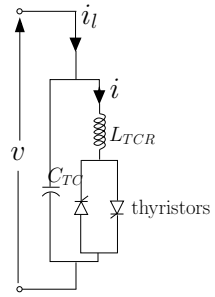

Fig. 1. SVC circuit diagram.

of v and i, respectively.

$$\begin{aligned} C_{TC}\frac{dV_1}{dt} &= I_l - I_1 - j\omega_0 C_{TC} V_1 \\ L_{TCR}\frac{dI_1}{dt} &= \langle qv \rangle_1 - j\omega_0 L_{TCR} I_1 \end{aligned} \quad (2)$$

The linearized model of the power system including SVC (without SSDC) is given by (3).

$$\Delta\dot{\underline{X}} = [A]\Delta\underline{X} \; + \; [B]\Delta\alpha \quad (3)$$

where $\underline{X}$ is the state vector.

III. SSDC Design

A. SSDC Structure

Since the SVC voltage regulation function has little influence on the improvement of the power system damping [11], the SVC is assumed to be operating in fixed firing angle control (FFAC) with no voltage regulator action. However, a subsynchronous damping function is assumed with a controller structure as depicted in Fig. 2. The generator rotor speed deviation is used as the control signal for SSDC [14], [16], [19], [23].

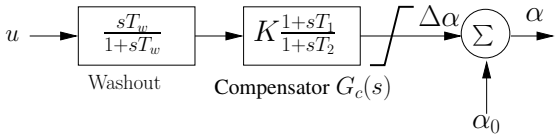

Fig. 2. SSDC for SVC.

B. Determination of the Phase-Frequency Characteristic

The phase angle through the generator (G), static VAR compensator (V), and power system (P) in the open-loop mode (i.e., without SSDC) is required to be determined. Equivalently, the transfer function $GVP(s)$ [$\frac{\Delta T_e(s)}{\Delta\alpha(s)}$] is to be computed. The phase response can be determined by substituting $s = j\omega$, with ω in the range of torsional mode frequencies. The procedure to obtain $GVP(s)$ using the proposed approach is outlined below.

The state-space model given in (3) is reduced to provide

$$\Delta\dot{\underline{X}}_R = [A_R]\Delta\underline{X}_R \; + \; [B_R]\Delta\alpha \quad (4)$$

where $\Delta\underline{X}_R$ denotes the state vector *excluding* the state variables of the mechanical system.

Writing the above equation in s-domain

$$\Delta\underline{X}_R(s) = \Big(sI - [A_R]\Big)^{-1}[B_R]\Delta\alpha(s) \quad (5)$$

The electromagnetic torque can be expressed as

$$\Delta T_e = [C_R]\Delta\underline{X}_R \quad (6)$$

Using (5) in (6), the desired transfer function $GVP(j\omega)$ is obtained as

$$GVP(j\omega) = \frac{\Delta T_e(j\omega)}{\Delta\alpha(j\omega)} = [C_R]\Big(j\omega I - [A_R]\Big)^{-1}[B_R] \quad (7)$$

Once the the phase response of the $GVP(j\omega)$ is determined, the compensator $G_c(s)$ is designed as follows [41]:

$$\beta \;=\; \frac{1-\sin\phi_t}{1+\sin\phi_t}, \quad T_1 = \frac{1}{\omega_t\sqrt{\beta}}, \quad T_2 = \beta T_1 \quad (8)$$

where ϕ_t is the compensator phase angle at the desired center frequency ω_t (rad/s). Design of the compensator should be such that the phase angle of the *compensated* $GVP(j\omega)$, which is equal to $\angle GVP(j\omega) + \angle SSDC(j\omega)$, is within $\pm 90^\circ$ in order to ensure positive electrical damping torque in the torsional mode frequency range [42].

IV. Case Studies

The case studies are carried out on the IEEE FBS [39]. The operating conditions are set as V_g=1.0 pu, E_b=1.0 pu, P_g=0.5 pu and x_{FC}=0.19 pu (38% of x_L). A single time constant static exciter is enabled on the generator. For this FSC compensation, the system is found to be SSR unstable as the frequency of the network subsynchronous mode is close to that of torsional mode-4 [43], —see the first column of Table I (without SVC).

Now, an SVC with B_L=0.075 pu and B_C=0.05 pu [case (a)] is connected at the generator terminals as shown in Fig. 3. Employing the SVC model presented in section II, the eigenvalues (for the nominal operating reactive power, Q_{s0}=0 pu, which corresponds to α_0=105.36°) are evaluated as indicated in the second column of Table I. From Table I it is observed that the SVC alone is insufficient for enhancement of the torsional modes damping and as a result, the system remains SSR unstable. An SSDC is, therefore, required for this purpose.

A detailed time-domain simulation is carried out in PSCAD/EMTDC to verify the eigen-inferences. With the SVC in service, the disturbance in the form of step reduction in the input mechanical torque at 3.5 s and clearing time of 0.075 s is considered. The simulation result is shown in Fig. 4. After the disturbance the shaft torque oscillation grows with time with the dominant frequency of 202 rad/s (see expanded view). This is in agreement with the eigenvalues given in Table I.

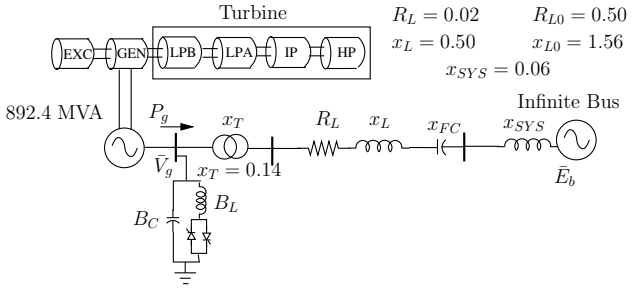

PLL (SVC voltage): $K_p = 144.34$ rad/s and $K_i = 57.74$ rad/s^2
Exciter: $K_A = 200$ pu/pu and $T_A = 0.025$ s

All data are in pu on generator MVA base

Fig. 3. The IEEE first benchmark model with an SVC.

TABLE I. MODES OF INTEREST (P_g=0.5 PU, x_{FC}=0.19 PU, B_L=0.075 PU, B_C=0.05 PU, α_0=105.36°)

without SVC	with SVC without SSDC	with SVC and SSDC (K=60)	Comments
-4.648± j553.55	-4.709± j553.55	-4.868± j553.48	Supersynchronous network mode
-4.524± j200.81	-4.602± j200.72	-3.405± j200.52	Subsynchronous network mode
1.096± j202.41	**1.068± j202.44**	**-0.135± j203.19**	**Torsional mode-4**
0.008± j160.72	0.007± j160.72	-0.011± j160.71	Torsional mode-3
0± j127.04	0± j127.04	-0.005± j127.04	Torsional mode-2
-0.017± j99.28	-0.017± j99.28	-0.061± j99.31	Torsional mode-1
-0.649± j9.52	-0.645± j9.51	-0.556± j9.41	Swing mode

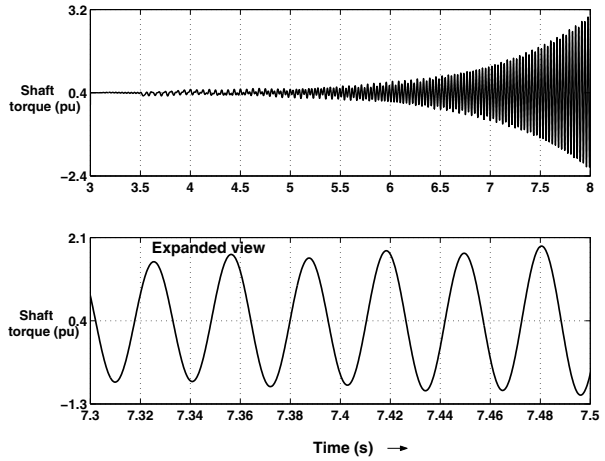

Fig. 4. Shaft torque between LPA and LPB turbines (P_g=0.5 pu, x_{FC}=0.19 pu, B_L=0.075 pu and B_C=0.05 pu) —without SSDC.

A. Determination of $GVP(j\omega)$ and Design of SSDC

The phase response of the $GVP(j\omega)$ is shown in Fig. 5. The figure also shows the phase angle of the $GVP(j\omega)$ obtained using the TS method. The CT model yields phase angles which are slightly higher than those of the TS method due to approximations made in the derivation of the CT model of SVC which is a highly non-linear device. Yet, the difference in the angles is mostly within 10° in the torsional frequency range, i.e., 100 to 205 rad/s. Further, in Fig. 5, the phase response of the $GVP(j\omega)$ for two more quiescent points such as Q_{s0}=+0.02 pu (inductive) and Q_{s0}=-0.02 pu (capacitive) are also given to show the effect of the operating point of the SVC on the $GVP(j\omega)$.

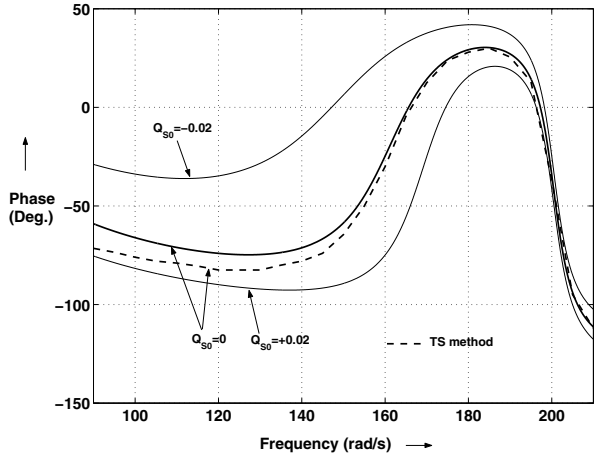

Fig. 5. Phase angle of $GVP(j\omega)$ (P_g=0.5 pu, x_{FC}=0.19 pu, B_L=0.075 pu and B_C=0.05 pu).

From the phase angles of the $GVP(j\omega)$, it is decided to design a lead compensator, $G_c(s)$, which offers a phase lead of ϕ_t=40° at the center frequency ω_t=300 rad/s. This is necessary to satisfy the ϕ_c-angle criterion (i.e., ϕ_c is between +90° and -90°) in the torsional frequency range. This resulted in the following transfer function:

$$G_c(s) = K\frac{(1 + s\ 0.007148)}{(1 + s\ 0.001554)} \tag{9}$$

An SSDC has been realized with this compensator in conjunction with a washout transfer function (T_w=5 s). The phase angle of the *compensated* $GVP(j\omega)$ is shown in Fig. 6.

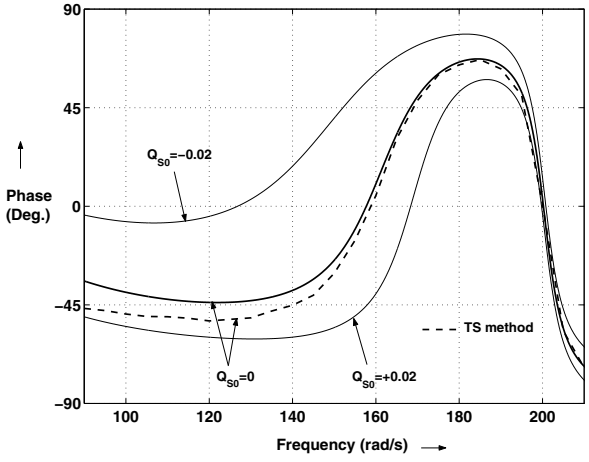

Fig. 6. Phase angle of the *compensated* $GVP(j\omega)$ (P_g=0.5 pu, x_{FC}=0.19 pu, B_L=0.075 pu and B_C=0.05 pu).

In order to decide the quiescent operating point, Q_{s0}, and the SSDC gain, K, Q_{s0} is varied and its effect on the torsional

mode-4 damping is studied. From the analysis, the quiescent operating point of the SVC is fixed at Q_{s0}=0 pu as it provides maximum damping and offers better utilization of the device ratings. It is noted that an increase in the gain of the SSDC deteriorates the damping of the subsynchronous network mode and the swing mode. Reduction of swing mode damping is not of major concern as it can be exclusively adjusted using a PSS. Therefore, for a good enough damping for the mode-4 and to stabilize all other torsional modes, K is chosen to be equal to 60.

For this gain, the eigenvalues obtained are listed in Table I. Evidently, all the torsional modes are stabilized using this SSDC. The simulation result shown in Fig. 7 for x_{FC}=0.19 pu validates the designed SSDC.

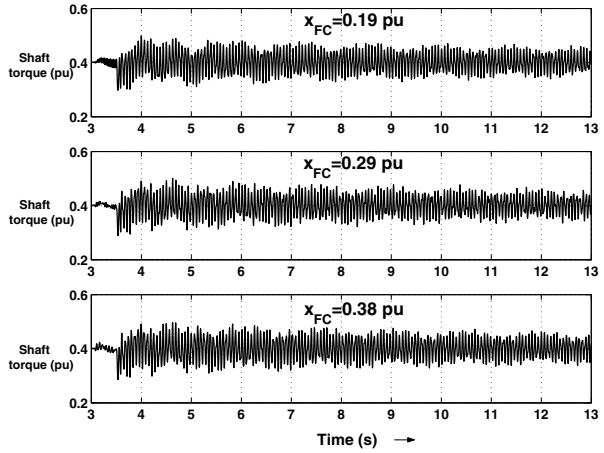

Fig. 7. Shaft torque between LPA and LPB turbines for P_g=0.5 pu and different x_{FC} (B_L=0.075 pu and B_C=0.05 pu) —with SSDC.

B. Higher Series Compensation Levels

In this section, the effectiveness of the proposed approach is examined at different series compensation levels. It is noted in [43] that the torsional modes have their largest SSR interaction at certain values of the FSC compensation. The critical compensation levels for the torsional modes-3 and -2 are x_{FC}=0.29 pu (58% of x_L) and 0.38 pu (76% of x_L), respectively. The lowest torsional mode, i.e., mode-1, is tuned only at a very high FSC compensation level (above 90% compensation) which is more unlikely to be employed in practice [44], [45]. Therefore, in this study, x_{FC}=0.46 pu (92% of x_L), the critical x_{FC} for mode-1 is not considered.

From Fig. 8 it can be seen that the GVP are different for different compensation levels. However, it is seen that the designed SSDC meets ϕ_c-angle criterion for all the FSC compensation levels as is evident from Fig. 9. The corresponding eigenvalues are listed in Table II. It is to be noted that the required gain differs for each of the FSC compensation level.

The simulation results obtained for different series compensation levels are shown in Fig. 7. From the figure, it can be seen that the designed SSDC stabilizes the system successfully at different critical x_{FC}. This study implies that the model provides reliable phase angles of $GVP(j\omega)$ over a wide range of series compensation.

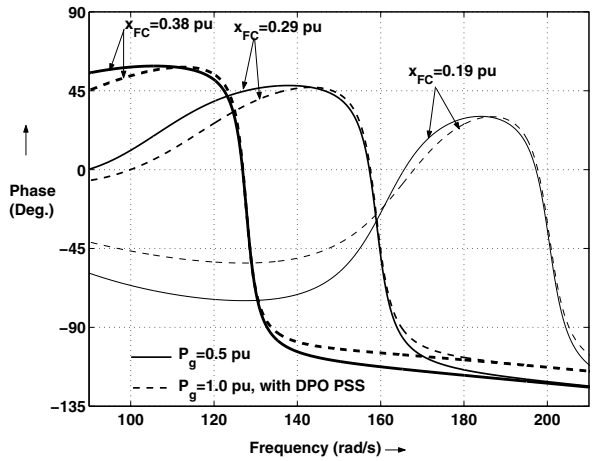

Fig. 8. Phase angle of the $GVP(j\omega)$ for different x_{FC} and P_g (B_L=0.075 pu and B_C=0.05 pu, Q_{s0}=0 pu).

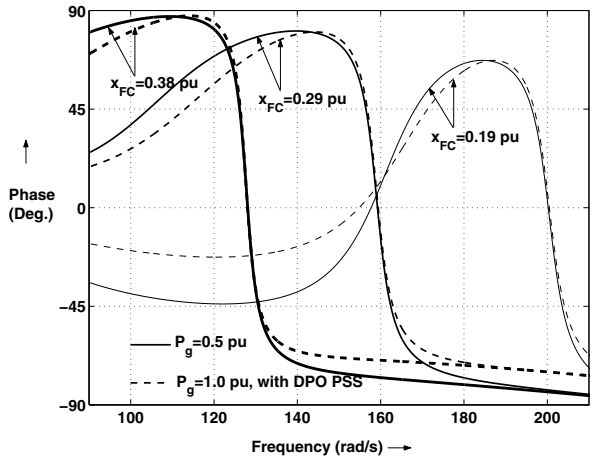

Fig. 9. Phase angle of the *compensated* $GVP(j\omega)$ for different x_{FC} and P_g (B_L=0.075 pu, B_C=0.05 pu, Q_{s0}=0 pu).

TABLE II. MODES OF INTEREST (P_g=0.5 PU, B_L=0.075 PU, B_C=0.05 PU AND Q_{s0}=0 PU)

x_{FC}=0.29 pu		x_{FC}=0.38 pu	
without SVC	with SVC and SSDC (K=85)	without SVC	with SVC and SSDC (K=140)
-4.689± j595.14	-5.036± j595.07	-4.717± j626.71	-5.284± j626.62
-4.036± j159.25	-2.820± j159.25	-2.790± j127.14	-2.196± j128.14
0.005± j202.81	-0.048± j203.34	-0.001± j202.87	-0.071± j203.63
1.207± j160.20	-0.171± j160.57	0.009± j160.43	-0.097± j160.93
0.003± j127.08	-0.002± j127.06	0.717± j127.07	-0.086± j126.86
-0.016± j99.49	-0.067± j99.45	0± j100.03	-0.044± j99.53
-0.817± j10.26	-0.672± j10.07	-1.009± j11.05	-0.752± j10.69

C. Higher Loading Levels

In this section, the $GVP(j\omega)$ is determined for P_g=1.0 pu (with Delta-P-Omega PSS [43]) and is compared against that obtained for P_g=0.5 pu —see Fig. 8. From the figure it can

be seen that the GVP differ by at most 20°, for any FSC compensation levels. Hence, the compensator $G_c(s)$ designed for P_g=0.5 pu is found to be adequate even for P_g=1.0 pu which is evident from Fig. 9. Through eigenvalue analysis, it is determined that P_g=1.0 pu operation requires gains of 56, 82.5 and 147.5 for x_{FC}=0.19 pu, 0.29 pu and 0.38 pu, respectively, to stabilize all the modes. These observations are verified through time-domain simulation as shown in Fig. 10. From this study it can be inferred that the proposed approach provides reliable phase angles of $GVP(j\omega)$ even at other loading conditions.

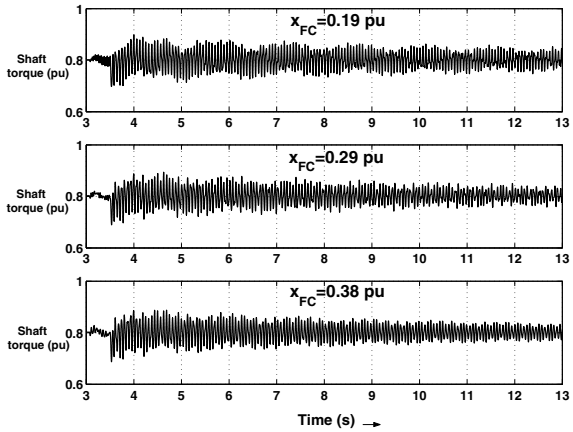

Fig. 10. Shaft torque between LPA and LPB turbines for P_g=1.0 pu and different x_{FC} (B_L=0.075 pu and B_C=0.05 pu) —with SSDC.

D. Performance of the SSDC for a Fault

The designed SSDC is investigated for its robustness by considering a single-line-to ground (LG) fault at the generator terminals at 3.5 s and cleared at 0.05 s. The operating condition is chosen such that P_g=1.0 pu, x_{FC}=0.38 pu. Fig. 11 shows that the system is unstable without the SSDC. On the other hand, the designed SSDC successfully stabilizes the system —see Fig. 12.

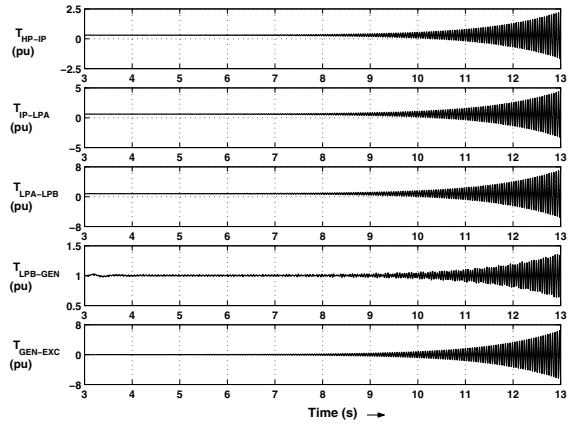

Fig. 11. The shaft torsional torques for an LG fault at the generator terminals —without SSDC.

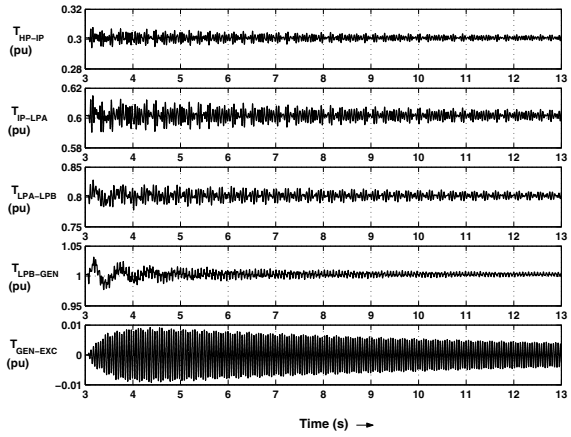

Fig. 12. The shaft torsional torques for an LG fault at the generator terminals —with SSDC.

V. Conclusions

In this paper, the use of a dynamic phasor model of SVC to obtain the phase response of a system, analytically, is demonstrated. Such an approach offers a way to design an SSDC reliably by employing the widely used PC approach. From the case studies it is seen that the phase angles obtained using the proposed approach are in close agreement with those obtained using the TS method. With the proposed method, the SSDC design becomes very straightforward for different series compensation levels and loading conditions.

In a TCSC-based SSR mitigation scheme [42], the compensator phase angle requirements were found to be quite different at different quiescent firing angles at higher series compensation levels, which in turn demand a multi-stage compensator-based SSDC. Since an SVC is a shunt device in comparison to TCSC, the level of FSC compensation does not greatly influence the typical frequency characteristic. Hence, SVC-based SSR mitigation scheme requires a simple single-stage SSDC for most of the FSC compensation levels.

The proposed approach can also be used to design SSDC for other FACTS devices such as STATCOM, SSSC, etc. Further, the method being general can be applied to large power system configurations as well. These studies will be taken up in the future work.

References

[1] K. R. Padiyar, *Analysis Of Subsynchronous Resonance In Power Systems*. Norwell, MA: Kluwer, 1999.

[2] K. Clark, "Overview of subsynchronous resonance related phenomena," in *Proc. IEEE/PES Transm. Distrib. Conf. and Exp.*, May 2012, pp. 1-3.

[3] Shashidhara Mecha Kotian, Adharapurapu Hema Latha and K. N. Shubhanga, "A Toy model to understand subsynchronous resonance and real-time simulation of the model using RTAI-Linux," in *Proc. IEEE Int. Conf. on Control, Instrumentation, Communication and Computational Technologies (ICCICCT 2015)*, Dec. 2015, pp. 66-73.

[4] X. Xie, L. Wang, and Y. Han, "Combined application of SEDC and GTSDC for SSR mitigation and its field tests," *IEEE Trans. Power Syst.*, vol. 31, no. 1, pp. 769-776, Jan. 2016.

[5] S. Wang, Z. Xu, and Shen Wang, "New findings on bypass damping filter in increasing subsynchronous resonance damping of series compensated system," *IET Gen. Trans. and Distrib.*, vol. 9, no. 3, pp. 1718-1726, Sep. 2015.

[6] X. Xie, P. Liu, K. Bai, and Y. Han, "Applying improved blocking filters to the SSR Problem of the Tuoketuo power system," *IEEE Trans. Power Syst.*, vol. 28, no. 1, pp. 227-235, Feb. 2013.

[7] R. K. Varma and S. Auddy, "Mitigation of subsynchronous resonance by SVC using PMU-acquired remote generator speed," in *Proc. IEEE Power India Conf.*, 2006, pp. 1-8.

[8] R. K. Varma, S. Auddy, and Y. Semsedini, "Mitigation of subsynchronous resonance in a series-compensated wind farm using FACTS controllers," *IEEE Trans. Power Del.*, vol. 23, no. 3, pp. 1645-1654, Jul. 2008.

[9] F. C. Jusan, S. Gomes, and G. N. Taranto, "SSR results obtained with a dynamic phasor model of SVC using modal analysis," *Int. J. Elect. Power Energy Syst.*, vol. 32, no. 6, pp. 571-582, Jul. 2010.

[10] O. Wasynczuk, "Damping subsynchronous resonance using reactive power control," *IEEE Trans. Power App. Syst.*, vol. 100, no. 3, pp. 1096-1104, Mar. 1981.

[11] R. M. Mathur and R. K. Varma, *Thyristor-Based FACTS Controllers for Electrical Transmission Systems*. New York: IEEE Press, 2002.

[12] Kakimoto and A. Phongphanphanee, " Subsynchronous resonance damping control of thyristor-controlled series capacitor," *IEEE Trans. Power Del.*, vol. 18, no. 3, pp. 1051-1059, Jul. 2003.

[13] L. A. S. Pilotto, A. Bianco, F. W. Long, and A. A. Edris, " Impact of TCSC control methodologies on subsynchronous resonance oscillations," *IEEE Trans. Power Del.*, vol. 18, no. 1, pp. 243-252, Jan. 2003.

[14] L. Min, Z. Xiaoxin, and T. Fang, "Small signal analysis of subsynchronous torsional interactions with TCSC," in *Proc. Int. Conf. Electrical Engineering*, China, Jul. 2009, pp. 1-6.

[15] D. Rai, S. O. Faried, G. Ramakrishna, and A. Edris, "Hybrid series compensation scheme capable of damping subsynchronous resonance," *IET Gener. Transm. Distrib.*, vol. 4, no. 3, pp. 456-466, Mar. 2010.

[16] S. R. Joshi, E. P. Cheriyan, and A. M. Kulkarni, "Output feedback SSR damping controller design based on modular discrete-time dynamic model of TCSC," *IET Gener. Transm. Distrib.*, vol. 3, no. 6, pp. 561-573, Jun. 2009.

[17] S. Panda, A. K. Baliarsingh, S. Mahapatra and S. C. Swain, " Supplementary damping controller design for SSSC to mitigate sub-synchronous resonance," *Mechanical Systems and Signal Processing*, vol. 68-69, pp. 523-535, Feb. 2016.

[18] T. Rajaram, J. M. Reddy and Y. Xu, "Kalman Filter Based Detection and Mitigation of Subsynchronous Resonance with SSSC," *IEEE Trans. Power Syst.*, vol. 32, no. 2, pp. 1400-1409, Mar. 2017.

[19] A. Ghorbani, B. Mozaffaria, and A. M. Ranjbar, "Application of subsynchronous damping controller (SSDC) to STATCOM," *Int. J. Elect. Power Energy Syst.*, vol. 43, no. 1, pp. 418-426, Dec. 2012.

[20] R. K. Varma and R. Salehi, "SSR mitigation with a new control of PV solar farm as STATCOM (PV-STATCOM)," *IEEE Trans. Sustainable Energy*, vol. 8, no. 4, pp. 1473-1483, Oct. 2017.

[21] D. Koteswara Raju, Bhimrao S. Umre, Anjali S. Junghare and B. Chitti Babu, "Mitigation of subsynchronous resonance with fractional-order PI based UPFC controller," *Mechanical Systems and Signal Processing*, vol. 85, pp. 698-715, Feb. 2017.

[22] X. Zheng, J. Zhang, and Z. Xu, "A supplementary damping controller of TCSC for mitigating SSR," in *Proc. IEEE Power and Energy Society General Meeting*, Canada, Jul. 2009, pp. 1-5.

[23] Z. Xin and G. Shan, "Damping subsynchronous oscillation by static var compensator," in *Proc. Int. Conf. Electricity Distribution*, China, Sep. 2010, pp. 1-5.

[24] X. Zheng, J. Zhang, and C. Wang, "Active damping controller design for SSSC to mitigate subsynchronous resonance," in *Proc. IEEE Power and Energy Society General Meeting*, Jul. 2010, pp. 1-6.

[25] T. Fang and Z. Xiaoxin, "Parameter determination of supplementary subsynchronous damping controller with residue method," in *Proc. Int. Conf. Power System Technology*, Kunming, China, 2002, pp. 365-369.

[26] T. Fang and Z. Xiaoxin, "Determination of the parameters of TCSC controller with residue method," in *Proc. Int. Conf. Electrical Engineering (ICEE 1999)*, Hong Kong, 1999, pp. 135-138.

[27] K. Kabiri, S. Henschel, J. R. Marti, and H. W. Dommel, "A discrete state-space model for SSR stabilizing controller design for TCSC compensated systems," *IEEE Trans. Power Del.*, vol. 20, no. 1, pp. 466-473, Jan. 2005.

[28] L. Wang and Y. Hsu, "Damping of subsynchronous resonance using excitation controllers and static VAR compensations: a comparative study," *IEEE Trans. Energy Convers.*, vol. 3, no. 1, pp. 6-13, Mar. 1988.

[29] Y. Hsu and C. Wu, "Design of PID static VAR controllers for the damping of subsynchronous oscillations," *IEEE Trans. Energy Convers.*, vol. 3, no. 2, pp. 210-216, Jun. 1988.

[30] L. Wang, S. J. Mau, and C. C. Chuko, "Suppression of common torsional mode interactions using shunt reactor controllers," *IEEE Trans. Energy Convers.*, vol. 8, no. 3, pp.539-545, Sep. 1993.

[31] S. Lee and C. Liu, "Damping subsynchronous resonance using a SIMO shunt reactor controller," *IEEE Trans. Power Syst.*, vol. 9, no. 3, pp. 1253-1262, Aug. 1994.

[32] K. R. Padiyar and Nagesh Prabhu, "Design and performance evaluation of subsynchronous damping controller with STATCOM," *IEEE Trans. Power Del.*, vol. 21, no. 3, pp. 1398-1405, Jul. 2006.

[33] M. Farahani, "Damping of subsynchronous oscillations in power system using static synchronous series compensator," *IET Gener. Transm. Distrib.*, vol. 6, no. 6, pp. 539-544, Jun. 2012.

[34] T. Yang, X. Xie, S. Liu, and D. Zhang, "Optimal design of SVC-based subsynchronous damping control using genetic and simulated annealing algorithm," in *Proc. Int. Conf. Information and Automation*, Zhangjiajie, China, 2008, pp. 1015-1020.

[35] S. R. Joshi and A. M. Kulkarni, "Analysis of SSR performance of TCSC control schemes using a modular high bandwidth discrete-time dynamic model," *IEEE Trans. Power Syst.*, vol. 24, no. 2, pp. 840-848, May 2009.

[36] D. Jovcic and G. N. Pillai, "Analytical modeling of TCSC dynamics," *IEEE Trans. Power Del.*, vol. 20, no. 2, pp. 1097-1104, Apr. 2005.

[37] D. Jovcic, N. Pahalawaththa, M. Zavahir, and H. A. Hassan, "SVC dynamic analytical model," *IEEE Trans. Power Del.*, vol. 18, no. 4, pp. 1455-1461, Oct. 2003.

[38] J. E. R. Alves, L. A. S. Pilotto, and E. H. Watanabe, "Thyristor-controlled reactors nonlinear and linear dynamic analytical models," *IEEE Trans. Power Del.*, vol. 23, no. 1, pp. 338-346, Jan. 2008.

[39] IEEE SSR Task Force, "First benchmark model for computer simulation of subsynchronous resonance," *IEEE Trans. Power App. Syst.*, vol. PAS-96, no. 5, pp. 1565-1572, Sep./Oct. 1977.

[40] Shashidhara Mecha Kotian and K. N. Shubhanga, "Dynamic Phasor Modelling and Simulation," in *Proc. IEEE India Conference (INDICON)*, 2015, pp. 1-6.

[41] K. Ogata, *Modern control engineering*. New Jersy: Prentice-Hall, 2001.

[42] Shashidhara Mecha Kotian and K. N. Shubhanga, "Design of a Subsynchronous Damping Controller Using a Dynamic PhasorBased Model of TCSC," in *Proc. IEEE International Conference on Power & Energy Systems: Towards Sustainable Energy (PESTSE)*, 2016, pp. 1-6.

[43] Shashidhara M. Kotian and K. N. Shubhanga, "Performance of synchronous machine models in a series-capacitor compensated system," *IEEE Trans. Power Syst.*, vol. 29, no. 3, pp. 1023-1032, May 2014.

[44] R. Grunbaum and J. Samuelsson, "Series capacitors facilitate long distance AC power transmission," in *Proc. IEEE Power Tech*, Russia, Jun. 2005, pp. 1-6.

[45] L. Wang and C. H. Lee, "Damping of subsynchronous resonance using modal-control NGH SSR damping scheme part II: two-machine common-mode study," in *Proc. TENCON'93*, Beijing, China, 1993, pp. 115-118.